

## Djurleite, digenite, and chalcocite: Intergrowths and transformations

MIHÁLY PÓSFAL, PETER R. BUSECK

Departments of Geology and Chemistry, Arizona State University, Tempe, Arizona 85287-1404, U.S.A.

### ABSTRACT

Intergrowths between djurleite ( $\sim\text{Cu}_{1.94}\text{S}$ ) and digenite ( $\sim\text{Cu}_{1.8}\text{S}$ ) and between djurleite and chalcocite ( $\text{Cu}_2\text{S}$ ) and the transformation between djurleite (dj) and chalcocite (cc) were studied using high-resolution transmission electron microscopy.

Pseudo-hexagonal twins are common in djurleite; crystal blocks are rotated relative to each other around [100], the normal of the close-packed layers, by multiples of  $60^\circ$ . Djurleite and digenite (dg) bands are intergrown, with  $(111)_{\text{dg}}$  parallel to  $(100)_{\text{dj}}$ , thereby creating a cubic-hexagonal alternation in the sequence of close-packed layers. The typical orientational relationship between coexisting djurleite and chalcocite is where  $[001]_{\text{cc}}$  is parallel to  $[100]_{\text{dj}}$  and  $[010]_{\text{cc}}$  is parallel to one of the  $\langle 010 \rangle$  or  $\langle 012 \rangle$  directions of djurleite.

If both djurleite and chalcocite occur in a sample, chalcocite easily converts to djurleite under the electron beam through the rearrangement of Cu atoms. A similar electrochemical transformation probably takes place in  $\text{Cu}_2\text{S}$ -CdS solar cells and is the reason for the instability of chalcocite in such devices.

### INTRODUCTION

Copper sulfides are widespread and are major sources of Cu. Digenite, djurleite, and chalcocite are the Cu-rich members of a series of minerals with compositions ranging from CuS (covellite) to  $\text{Cu}_2\text{S}$  (chalcocite) (Table 1). Djurleite was discovered as a mineral by Roseboom (1962), following its synthesis by Djurle (1958). Since chalcocite and djurleite are not readily distinguished from each other by optical methods (Ramdohr, 1980), relatively little is known about their orientational relationships and intergrowths. However, knowledge of such relationships is useful for understanding phase relations, transformations, and reactions of copper sulfides.

Besides being an important ore mineral, chalcocite has an important materials science application in the  $\text{Cu}_2\text{S}$ -CdS couple in solar cells (Te Velde and Dieleman, 1973). Copper sulfide solar cells were considered in the 1970s and 1980s as inexpensive replacements for costly Si cells. However, a distinct problem with chalcocite cells is that they proved to be unstable over time (Moitra and Deb, 1983).

Low-temperature chalcocite and djurleite have complex hexagonal close-packed structures with large unit cells (chalcocite: space group  $P2_1/c$ ,  $a = 1.525$ ,  $b = 1.188$ ,  $c =$

$1.349$  nm,  $\beta = 116.35^\circ$ ; djurleite: space group  $P2_1/n$ ,  $a = 2.690$ ,  $b = 1.575$ ,  $c = 1.357$  nm,  $\beta = 90.13^\circ$ ) (Evans, 1979). The structure of digenite is based on an antifluorite-type subcell in which the close-packed Cu + S layers follow a cubic stacking scheme (Donnay et al., 1958; Morimoto and Kullerud, 1963). The clustering of vacancies and Cu atoms produces several types of digenite superstructures (Pierce and Buseck, 1978; Conde et al., 1978).

The phase relations of the copper sulfides have been studied extensively. Monoclinic chalcocite converts to a high-temperature hexagonal polymorph at  $103^\circ\text{C}$ , and the upper limit of stability of djurleite is  $93^\circ\text{C}$  (Roseboom, 1966; Mathieu and Rickert, 1972; Potter, 1977). According to Morimoto and Koto (1970) and Morimoto and Gyobu (1971), digenite is stable at room temperature only if it contains a small amount of Fe.

The goals of this paper are to investigate the microstructures of natural samples of chalcocite, djurleite, and digenite in order to obtain a better understanding of their relationships and to obtain insights into the processes that take place in  $\text{Cu}_2\text{S}$ -CdS solar cells and that make them unstable. We used high-resolution transmission electron microscopy (HRTEM) so that we could obtain simultaneous structural and textural information.

TABLE 1. Compositions, structures, and stabilities of Cu-rich copper sulfide minerals

Mineral	Composition	S packing	System	Stability	References
Chalcocite (low)	$\text{Cu}_{1.99-2}\text{S}$	hcp	monoclinic	$T < 103^\circ\text{C}$	Roseboom (1966)
Chalcocite (high)	$\text{Cu}_{1.96-2}\text{S}$	hcp	hexagonal	$\sim 103^\circ\text{C} < T < \sim 435^\circ\text{C}$	Roseboom (1966)
Chalcocite (high- <i>P</i> )	$\text{Cu}_2\text{S}$	ccp	tetragonal	$1 \text{ kbar} < P, T < 500^\circ\text{C}$	Skinner (1970)
Djurleite	$\text{Cu}_{1.93-1.96}\text{S}$	hcp	monoclinic	$T < 93^\circ\text{C}$	Potter (1977)
Digenite (low)	$\text{Cu}_{1.75-1.8}\text{S}$	ccp	cubic	metastable	Morimoto and Koto (1970)
Digenite (high)	$\text{Cu}_{1.73-2}\text{S}$	ccp	cubic	$83^\circ\text{C} < T$	Roseboom (1966)
Anilite	$\text{Cu}_{1.75}\text{S}$	ccp	orthorhombic	$T < 72^\circ\text{C}$	Morimoto et al. (1969)

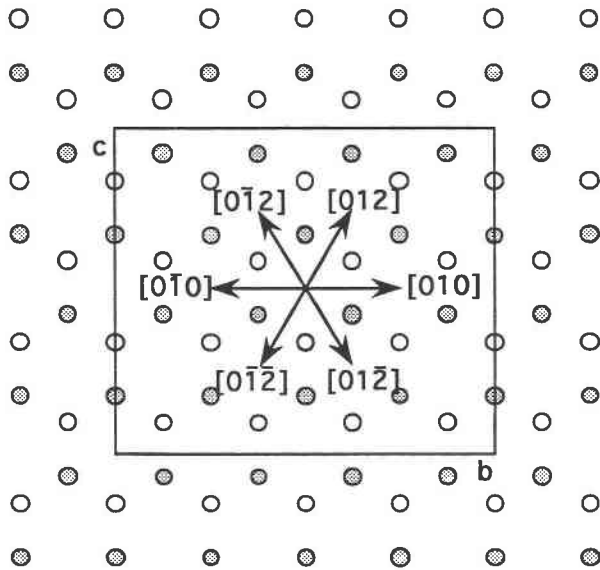


Fig. 1. Explanation of the pseudohexagonal twinning of djurleite. The open and shaded circles represent two layers of S atoms; a djurleite unit cell is outlined. The arrows represent pseudohexagonal axes indexed on the monoclinic djurleite cell. In twinned djurleite, individual crystals are rotated around  $[100]$  by multiples of  $60^\circ$  relative to one another.

### EXPERIMENTAL

We studied djurleite from the Dome Rock Mountains, Arizona, and chalcocite from Redruth, Cornwall (inventory nos. N-067 and A-820 at Eötvös Loránd University Mineral Collection, Budapest). Specimens for HRTEM studies were prepared both by ion-beam milling and by crushing the minerals gently in an agate mortar under chloroform and dispersing the particles onto holey car-

bon films supported by Cu grids. Since we noticed that ion milling induces transformations in djurleite and chalcocite, the preferred method of specimen preparation was grinding. In this paper only the micrograph of coherently intergrown chalcocite and djurleite (discussed in the next section and labeled Figure 6) was obtained from an ion-milled sample; all other figures present results from crushed minerals.

Electron microscopy was performed with a JEOL 4000EX electron microscope at a 400-kV operating voltage ( $C_s = 1.0$  mm), using a top-entry, double-tilt ( $x, y = \pm 20^\circ$ ) goniometer stage.

### OBSERVATIONS

#### Djurleite twinning

Twinning in djurleite is so common that it long hampered a structure determination (Evans, 1979). The twin laws operating on djurleite were identified by Takeda et al. (1967), who distinguished between pseudohexagonal and pseudotetragonal twins.

Pseudohexagonal twins occur in many crystals in the djurleite sample we studied. Sectors are rotated relative to one another by multiples of  $60^\circ$  around  $[100]$ , which is perpendicular to the hexagonal close-packed planes. Figure 1 displays two S layers of the djurleite structure. The hexagonal symmetry of the S framework is reduced to monoclinic by the arrangement of the Cu atoms. Selected-area electron-diffraction (SAED) patterns taken along the  $\langle 010 \rangle$  and  $\langle 012 \rangle$  zone axes are easily distinguished (Fig. 2a, 2b). If the crystal is twinned and contains both  $\langle 010 \rangle$ - and  $\langle 012 \rangle$ -type domains, a composite diffraction pattern like that in Figure 2c is obtained. Twinned djurleite crystals may contain as many as six distinct individuals; however, since the  $\beta$  angle deviates from  $90^\circ$  by only  $0.13^\circ$ , it is difficult to identify more than

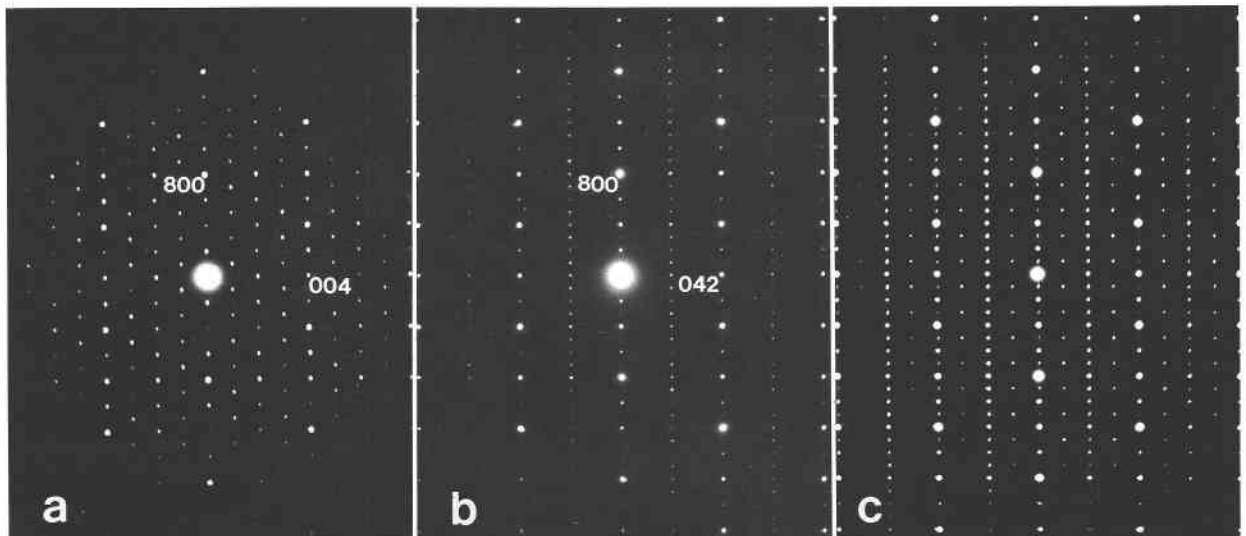


Fig. 2. SAED patterns of djurleite taken from directions perpendicular to  $[100]$ . (a) The  $[010]$  projection, (b)  $[01\bar{2}]$  projection, (c) twinned djurleite. Pattern c is a composite of a and b.

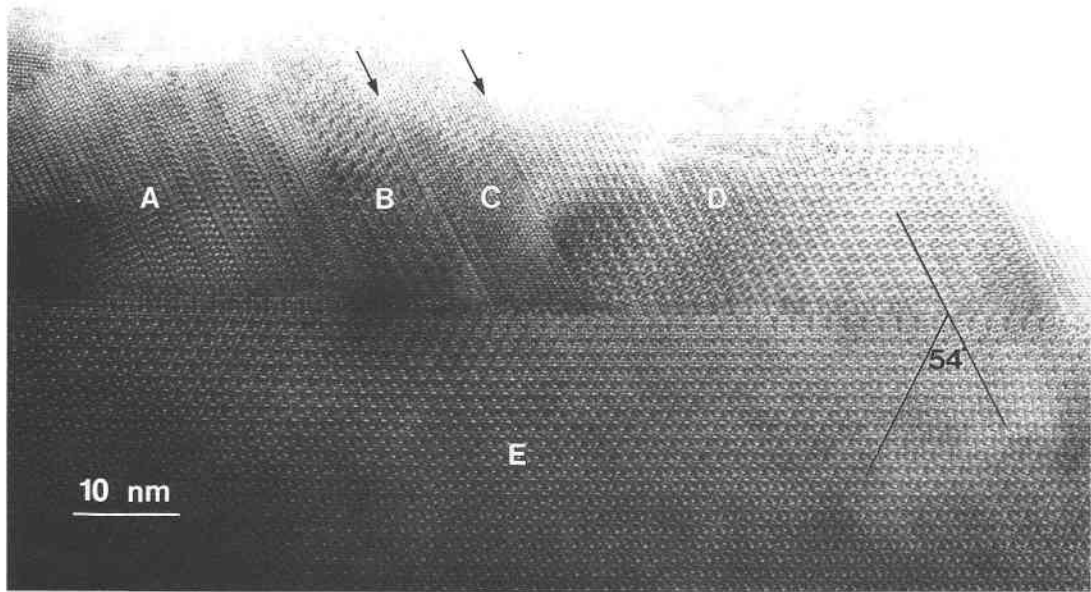


Fig. 3. Domains in djurleite. A, B, C, and D are pseudo-hexagonal twins. Domain A is viewed along a [012]-type direction, whereas B, C, and D are all viewed along [010]-type directions. The arrows mark contrast changes that suggest that B and D are in the same orientation, but C is rotated by 180° around [100] relative to B and D (e.g., if B and D are [010], then C is [0 $\bar{1}$ 0]).

two individuals from SAED pattern like the one in Figure 2c. In addition to 60° twins, other types of rotation domains also occur (Fig. 3).

#### Djurleite-digenite intergrowths

Narrow strips having disordered stacking sequences commonly occur between djurleite twin individuals. Al-

though from the image alone it is difficult to assign a particular mineral name to the area marked dg [110] in Figure 4, the structural character and orientation of these units were confirmed from diffraction patterns computed from the digitized image. We identified the disordered bands between djurleite units in Figure 4 as digenite, with  $(111)_{dg} \parallel (100)_{dj}$ .

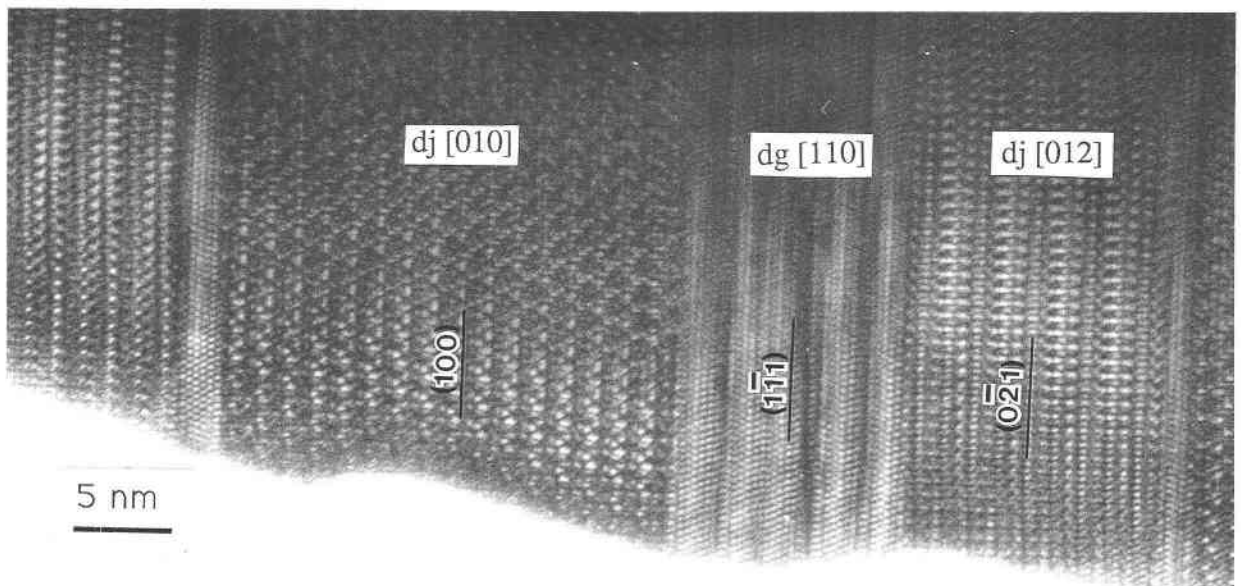


Fig. 4. Digenite (dg) bands in twinned djurleite (dj); the zone-axis indices mark the direction of projection for each structural unit.

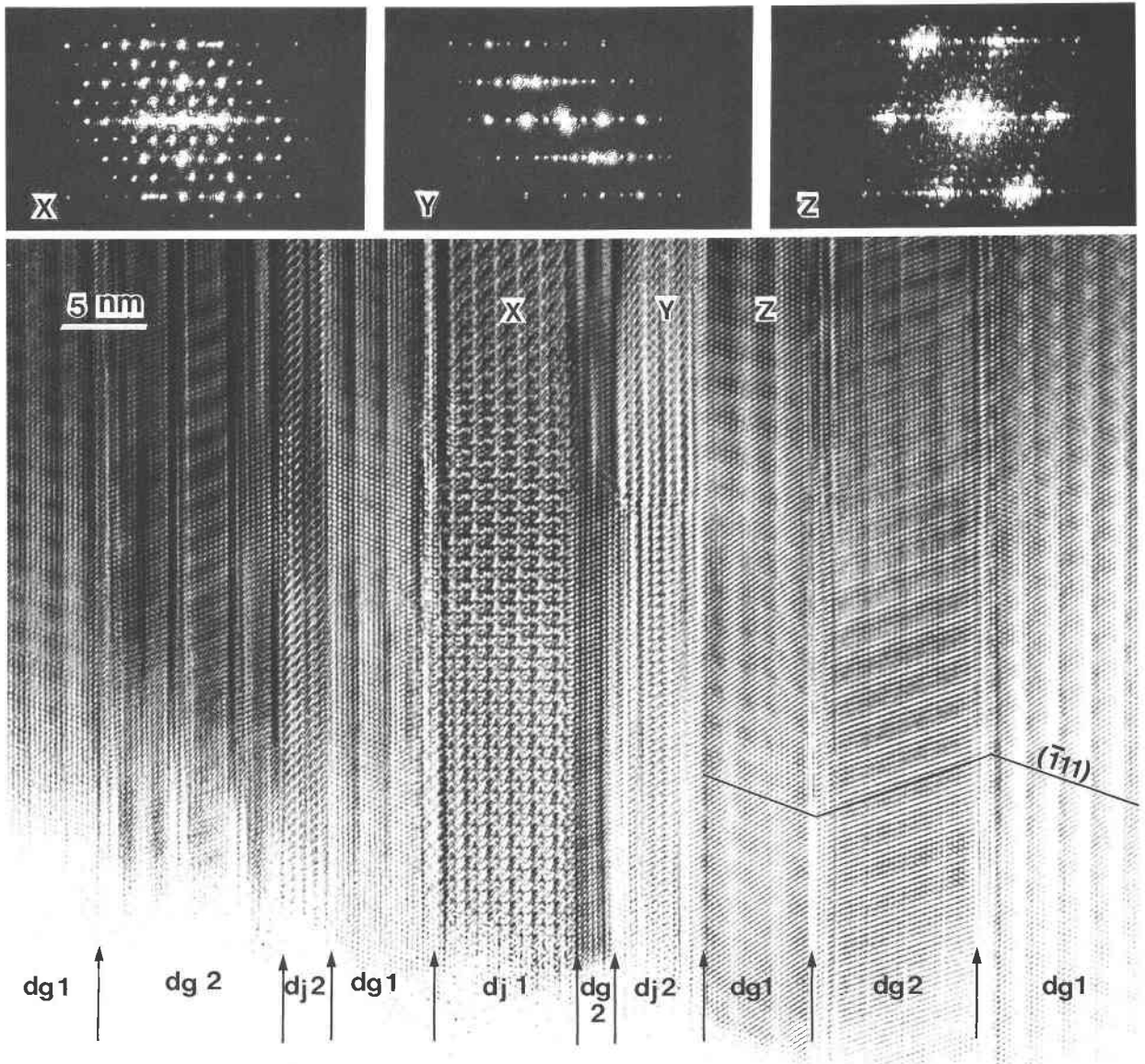


Fig. 5. Intergrowth of twinned digenite with twinned djurleite. The arrows mark boundaries between structural units. The 1 and 2 refer to the crystal blocks in a twin relation to each other. The diffraction patterns were computed from the digitized micrograph; the particular structural units to which they belong are marked on the micrograph. X: djurleite in [010] projection, Y: djurleite in [012] projection, Z: 6a-type digenite in [110] projection.

Larger blocks of digenite also occur in djurleite. The twinned slabs of digenite in Figure 5 basically have the 6a-type superstructure (see the computed diffraction pattern marked Z in Fig. 5). The digenite bands are a few unit cells thick and are separated either by twin boundaries or by slabs of djurleite that is itself twinned. The crystal in Figure 5 exhibits a wide variety of structural features: (1) ordering of vacancies and Cu atoms that produces the digenite 6a-type superstructure (Conde et al., 1978; Pierce and Buseck, 1978), as seen on the diffraction pattern marked Z, (2) 180° rotation twinning around [111] in digenite that introduces stacking faults into the cubic sequence of close-packed layers [see the change in ori-

entation of the line denoting the  $(\bar{1}11)$  plane on the right side of the figure], (3) 60° rotation twinning in djurleite, as indicated by the diffraction patterns marked X and Y, and (4) alternation of cubic close-packed (digenite) and hexagonal close-packed (djurleite) stacking sequences.

#### Djurleite and chalcocite

The Cornwall sample that we studied consists of chalcocite and djurleite. We found that the method used for specimen preparation affects the outcome of the TEM study. Although we could obtain high-resolution images from chalcocite when looking at ion-beam milled specimens, we were not able to obtain similar micrographs

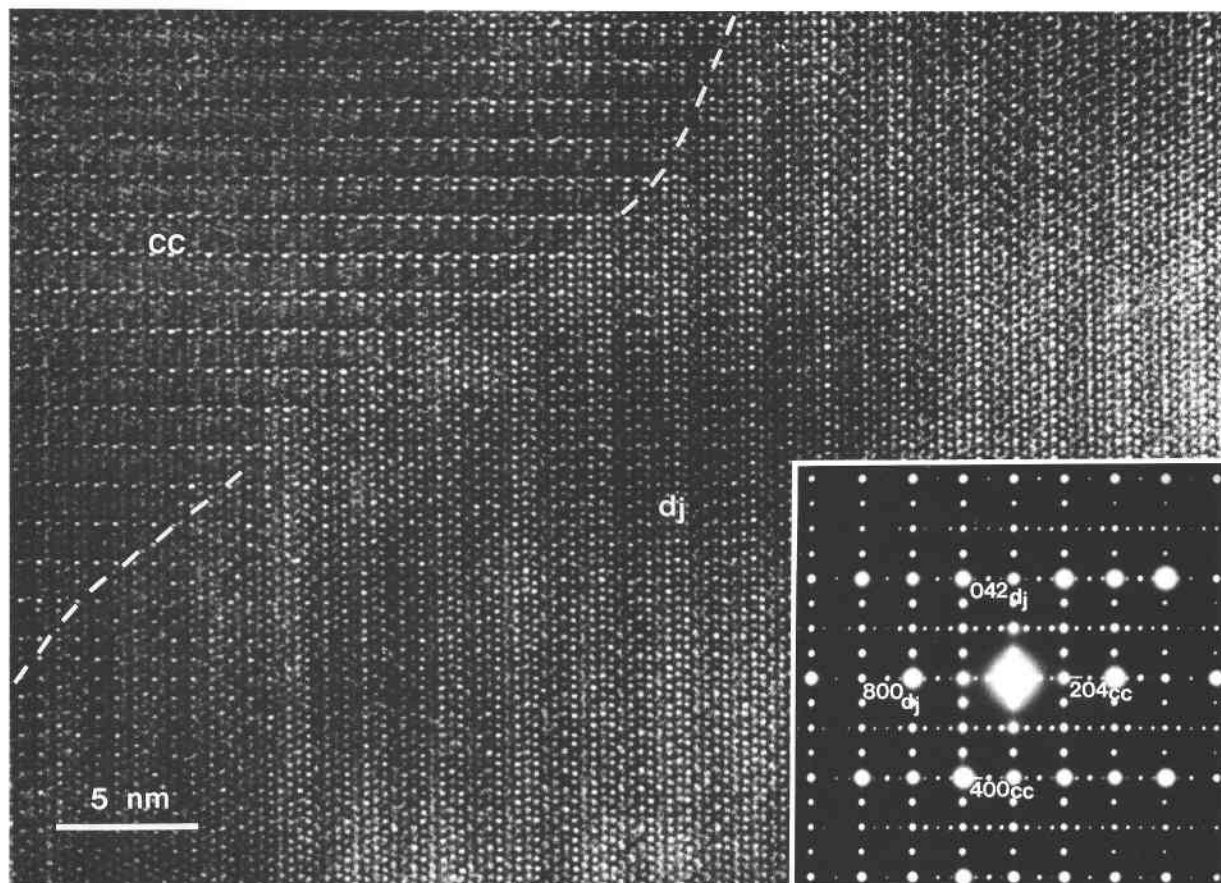


Fig. 6. Coherently intergrown chalcocite and djurleite in an ion-milled sample (cc: chalcocite viewed down  $[010]$ ; dj: djurleite viewed down  $[01\bar{2}]$ ).

using specimens that were ground in an agate mortar. Crushed grains of chalcocite typically converted to djurleite when exposed to an electron beam strong enough to readily produce high-resolution images (at a beam current of  $\sim 14$  pA/cm<sup>2</sup>, as measured on the viewing screen of the microscope).

On the other hand, specimens thinned by ion-beam milling may not reflect the original relationship between chalcocite and djurleite crystals in the sample. Heating the specimen to 190 °C during embedding and then bombarding it with Ar ions converted djurleite into chalcocite and high digenite. After being cooled to room temperature and stored for several months, part of the material reverted to djurleite. In such specimens, intergrowths of djurleite and chalcocite were stable in the electron beam, and  $[010]_{cc}$  was commonly parallel to one of the pseudo-hexagonal axes ( $\langle 010 \rangle$  or  $\langle 012 \rangle$ ) of djurleite, with  $[001]_{cc} \parallel [100]_{dj}$  (Fig. 6).

Although high-resolution images are not available from crushed grains of chalcocite, SAED patterns confirm that in unaltered natural samples chalcocite is typically intergrown with djurleite in the same fashion as is seen in Figure 6. This orientational relationship allows the close-packed S layers to be continuous across the interface; only

the Cu atoms are in different positions on the two sides of the boundary. Figure 7 demonstrates this relationship by displaying the structures of chalcocite and djurleite as projected along the pseudo-hexagonal axes of the S layers.

When chalcocite converts to djurleite under the electron beam, the framework of S atoms remains intact; only the Cu atoms rearrange. Such transformations were reported by Putnis (1977). In addition to the reversible chalcocite  $\leftrightarrow$  djurleite transformation, we observed that the movement of Cu atoms also produces conversions directly between different djurleite orientations. Figure 8 provides an example of how four different SAED patterns could be obtained from the same crystal while it was exposed for several minutes to the electron beam, but retained in one position throughout the experiment. First we recorded the pattern in Figure 8a (chalcocite  $[100]$ ); then the three SAED patterns corresponding to djurleite (Fig. 8b–8d) were observed in sequence within a few minutes. The four patterns appeared and disappeared in cycles and in an apparently random fashion, except that the chalcocite pattern only occurred when a low ( $< 10$  pA/cm<sup>2</sup>) electron-beam current was used. The S sublattice remains invariant during conversions among chalcocite  $[100]$ , djurleite  $[132]$ ,  $[104]$ , and  $[\bar{1}32]$ . The orientational

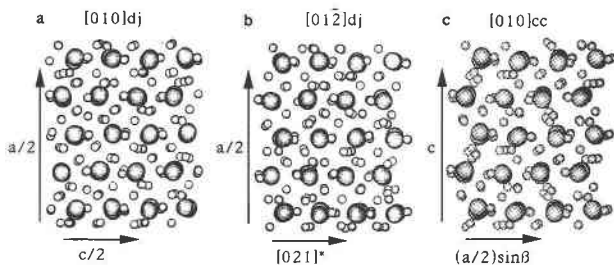


Fig. 7. The structure of djurleite as viewed along (a)  $[010]_{dj}$  and (b)  $[01\bar{2}]_{dj}$ . (c) The structure of chalcocite as viewed from  $[010]$ . Large circles: S atoms; small circles: Cu atoms. Parts b and c display the orientations present in Fig. 6, where the two domains contain S atoms in identical positions, but Cu atoms are in different arrangements.

relationship between chalcocite and djurleite in Figure 8 is the same as that found in ion-beam milled specimens, and the three orientations of djurleite are in (pseudo-hexagonal) twin relations to one another.

High-resolution images provide insight into the transformation mechanisms. Spectacular changes could be observed in real time on the TV screen that was connected to the electron microscope. When the Cu atoms began to move, the sharp image gradually became blurred; after a few seconds no details could be seen in the image. After 10–20 s, sharp, ordered spots abruptly appeared on the screen, but their arrangement indicated an orientation different from the previous one. Between certain stages of the transformation cycle the process did not go to completion in one step; first, only a part (the left side) of the crystal converted to the other orientation (Fig. 9). Figure 10 displays two stages of the transformation from  $[132]_{dj}$  to  $[104]_{dj}$  orientation: (1) part of the crystal converted to the  $[104]_{dj}$  orientation (Fig. 10a), and then (2) the entire crystal switched to  $[104]_{dj}$ , but the previous orientation boundary was preserved as an antiphase boundary (Fig. 10b). In order to obtain images of different parts of a large grain, the crystal was translated under the electron beam, causing uneven exposure to the electron irradiation. This procedure may have been responsible for the separate nucleation events observed in the transformation process.

## DISCUSSION

The Arizona djurleite sample contains both fault-free and heavily twinned crystals. Intergrowths with disordered 6a-type digenite are associated with the defective djurleite crystals. As discussed by Veblen (1992), HRTEM studies tend to emphasize pathological disorder in minerals, although it may also be important to know whether ordered structures occur in a particular sample. In the case of the djurleite sample, the large number of defect-free grains suggests that structural disorder is a local phenomenon.

According to Potter (1977), djurleite forms with digenite if the value of Cu/S is between 1.79 and 1.93. Djur-

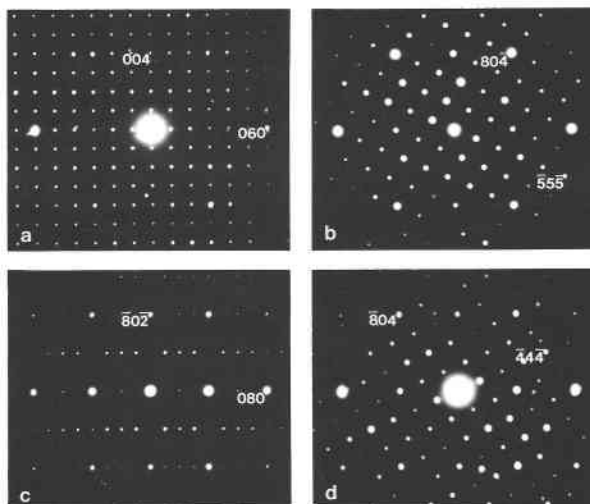


Fig. 8. Transformations between one chalcocite orientation and three djurleite orientations, as observed under the electron beam. (a) Chalcocite  $[100]$ , (b) djurleite  $[132]$ , (c) djurleite  $[104]$ , (d) djurleite  $[132]$ . (See text for discussion.)

leite coexists with digenite in a sample from the Magma mine, Arizona (Morimoto and Gyobu, 1971), and Morimoto and Koto (1970) synthesized 6a-type digenite with the composition of  $\text{Cu}_{1.80}\text{S}$ . However, several studies indicate that digenite is not stable at room temperature (Potter, 1977; Morimoto and Gyobu, 1971; Putnis, 1977); instead anilite ( $\text{Cu}_{1.75}\text{S}$ ) is the stable mineral occurring with djurleite (Table 1). Furthermore, Morimoto et al. (1969) found that grinding samples that contained both anilite and djurleite produced digenite. However, we ground our samples gently and djurleite was preserved,

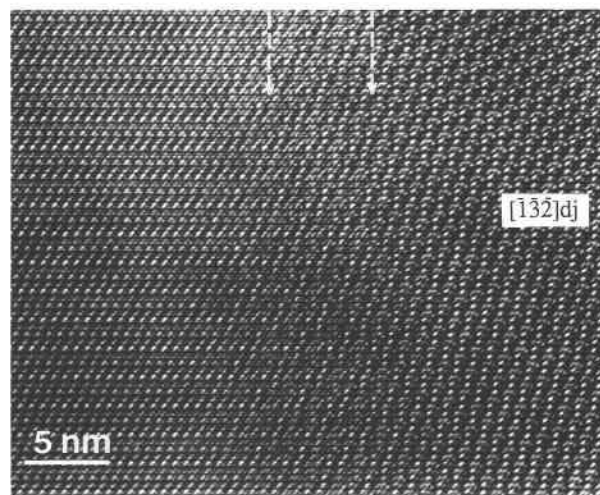


Fig. 9. HRTEM image of a fuzzy grain boundary (marked by arrows) between djurleite  $[104]$  and djurleite  $[132]$  orientations. The left part of the image corresponds to the SAED pattern in Fig. 8c and the right part to Fig. 8d.

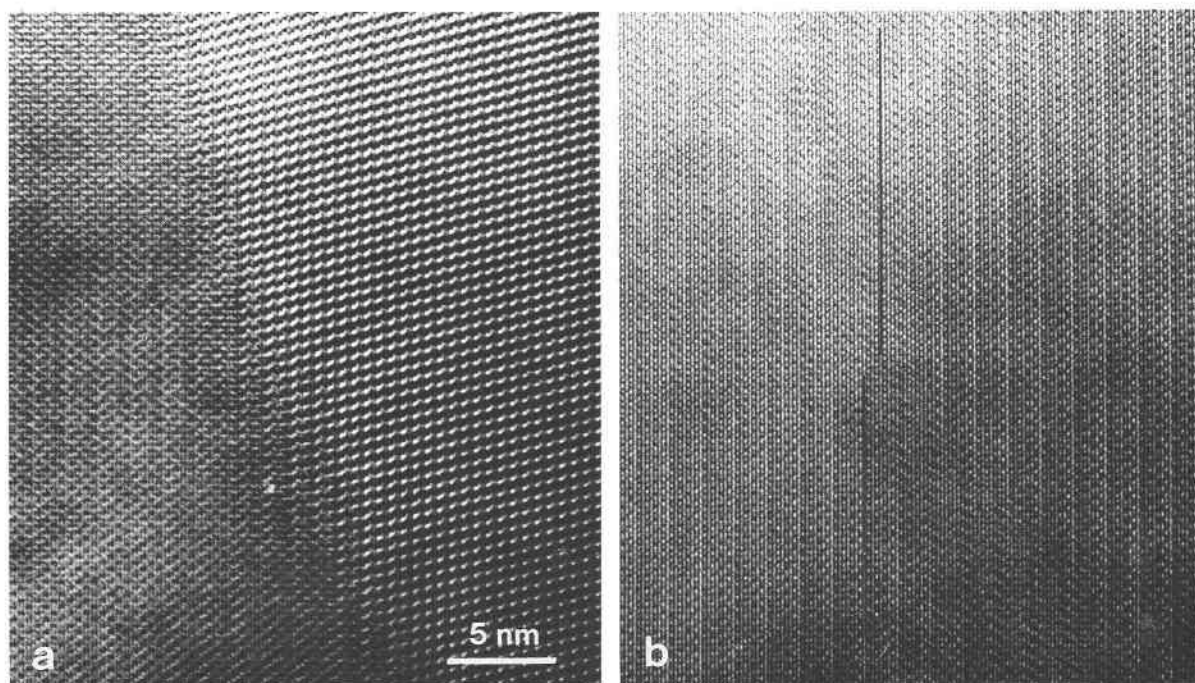


Fig. 10. Two stages in the transformation of a crystal from djurleite [132] into djurleite [104] orientations. (a) The left part of the image converted into the [104] orientation, but the right part is still in [132] orientation. (b) After a few seconds the right part has also converted into the [104] orientation. The previous grain boundary is preserved as an antiphase boundary.

and so we think that the electron micrographs showing intergrowths of djurleite and digenite reflect the original relationship of minerals in the sample.

The presence of untwinned djurleite crystals suggests a primary origin because djurleite crystals formed by solid-state transformation of high chalcocite would be heavily twinned (Evans, 1979). Apparently, changes in the Cu/S ratio of the ore-forming fluid controlled whether pure djurleite or assemblages of digenite and djurleite crystallized. It is likely that the sample that we studied formed between 72 and 93 °C (the upper limits of stability for anilite and djurleite, respectively; Potter, 1977; Morimoto and Koto, 1970); on cooling to room temperature the metastable 6a-type digenite could persist.

Our results confirm that if chalcocite and djurleite occur in the same sample, transformations between them are possible under the electron beam. The composition of djurleite extends from  $\text{Cu}_{1.93}\text{S}$  to  $\text{Cu}_{1.96}\text{S}$  (Potter, 1977). Djurleite and chalcocite coexist if the Cu/S ratio is between 1.96 and 2 (Potter, 1977). Based on his TEM observations, Putnis (1977) suggested that the composition ranges of chalcocite and djurleite overlap. If his suggestion is correct, then our results are compatible with an isochemical transformation. On the other hand, if the compositional values in Table 1 are correct, then the slight chemical differences are compensated by the diffusion of Cu atoms to and from other crystals that were in contact with the crystal exposed to the electron beam. The reversibility of the transformations indicates that the loss

of S in the electron beam is not significant in our experiments.

Putnis (1977) attributed the chalcocite  $\leftrightarrow$  djurleite transformation to the heating effect of the electron beam. However, Leon (1990) showed that djurleite directly transforms into high chalcocite and high digenite on heating, without converting to monoclinic chalcocite. We did not observe the appearance of high chalcocite during our experiments, and djurleite crystals in the Arizona sample were stable in the beam under operating conditions similar to those used in the study of the Cornwall sample, suggesting that the temperature of the grains was not raised above 93 °C. Instead we assume that the transformations result from electrochemical reactions caused by the flow of electrons through the crystal. Changes in the electric current make the Cu atoms move and reorder to a scheme different from the previous arrangement. The Cu atoms switch their positions, not only alternatingly producing the djurleite and chalcocite structure, but also creating several orientational variants of djurleite. As Evans (1979) put it, "even nature has difficulty in finding a stable arrangement for them."

The chalcocite  $\leftrightarrow$  djurleite transformations that we observed in a natural sample could also occur in the copper sulfide layer of  $\text{Cu}_2\text{S}$ -CdS solar cells. When such solar cells are fabricated, conditions are optimized to obtain monoclinic chalcocite as the copper sulfide phase because chalcocite yields high efficiencies (Caswell et al., 1977). However, djurleite (Te Velde and Dieleman, 1973; Na-

kayama et al., 1971) and the high-pressure, tetragonal polymorph of chalcocite (Sands et al., 1984) were also detected in the copper sulfide layer. It was suggested by Putnis (1976) that the efficiency of the cell deteriorates if the chalcocite converts to djurleite. We propose that this transformation happens through an electrochemical reaction similar to what we observed in the electron microscope. Since solar cells are made with the purpose of producing electric current, electrons inevitably flow through the slightly Cu-deficient chalcocite and presumably convert it into djurleite.

#### ACKNOWLEDGMENTS

We thank István Dódonny for his helpful comments and suggestions. Reviews by Carl O. Moses and Eugene S. Ilton improved the manuscript. This study was supported by National Science Foundation (NSF) grant EAR-92-19376. This work is based upon research conducted with TEMs located in the Center for High Resolution Electron Microscopy, which is supported by the National Science Foundation under grant no. DMR-91-15680.

#### REFERENCES CITED

- Caswell, B.G., Russell, G.J., and Woods, J. (1977) The phase of  $\text{Cu}_2\text{S}$  in the  $\text{CdS-Cu}_2\text{S}$  photovoltaic cell. *Journal of Physics D: Applied Physics*, 10, 1345-1350.
- Conde, C., Manolikas, C., Van Dyck, D., Delavignette, P., Van Landuyt, J., and Amelinckx, S. (1978) Electron microscopic study of digenite-related phases ( $\text{Cu}_{2-x}\text{S}$ ). *Materials Research Bulletin*, 13, 1055-1063.
- Djurle, S. (1958) An x-ray study on the system Cu-S. *Acta Chemica Scandinavica*, 12, 1415-1426.
- Donnay, G., Donnay, J.D.H., and Kullerud, G. (1958) Crystal and twin structure of digenite,  $\text{Cu}_2\text{S}$ . *American Mineralogist*, 43, 230-242.
- Evans, H.T., Jr. (1979) The crystal structures of low chalcocite and djurleite. *Zeitschrift für Kristallographie*, 150, 299-320.
- Leon, M. (1990) The phase transition of djurleite thin films. *Journal of Materials Science*, 25, 669-672.
- Mathieu, H.J., and Rickert, H. (1972) Elektrokemisch-thermodynamische Untersuchungen am System Kupfer-Schwefel bei Temperaturen  $T = 15-90^\circ\text{C}$ . *Zeitschrift für Physikalische Chemie*, 79, 315-330.
- Moitra, K., and Deb, S. (1983) Degradation of the performance of  $\text{Cu}_2\text{S}/\text{CdS}$  solar cells due to a two-way solid state diffusion process. *Solar Cells*, 9, 215-228.
- Morimoto, N., and Gyobu, A. (1971) The composition and stability of digenite. *American Mineralogist*, 56, 1889-1909.
- Morimoto, N., and Koto, K. (1970) Phase relations of the Cu-S system at low temperatures: Stability of anilite. *American Mineralogist*, 55, 106-117.
- Morimoto, N., and Kullerud, G. (1963) Polymorphism in digenite. *American Mineralogist*, 48, 110-123.
- Morimoto, N., Koto, K., and Shimazaki, Y. (1969) Anilite,  $\text{Cu}_2\text{S}_4$ , a new mineral. *American Mineralogist*, 54, 1256-1268.
- Nakayama, N., Gyobu, A., and Morimoto, N. (1971) Electrochemical synthesis and photovoltaic effect of copper sulfides on CdS single crystals. *Japanese Journal of Applied Physics*, 10, 1415-1418.
- Pierce, L., and Buseck, P.R. (1978) Superstructuring in the bornite-digenite series: A high-resolution electron microscopy study. *American Mineralogist*, 63, 1-16.
- Potter, R.W., II (1977) An electrochemical investigation of the system copper-sulfur. *Economic Geology*, 72, 1524-1542.
- Putnis, A. (1976) The transformation behaviour of cuprous sulphides and its application to the efficiency of  $\text{Cu}_2\text{S-CdS}$  solar cells. *Philosophical Magazine*, 34, 1083-1086.
- (1977) Electron diffraction study of phase transformations in copper sulfides. *American Mineralogist*, 62, 107-114.
- Ramdohr, P. (1980) The ore minerals and their intergrowths (2nd edition), 1207 p. Pergamon, Oxford, England.
- Roseboom, E.H., Jr. (1962) Djurleite,  $\text{Cu}_{1.96}\text{S}$ , a new mineral. *American Mineralogist*, 47, 1181-1184.
- (1966) An investigation of the system Cu-S and some natural copper sulfides between  $25^\circ$  and  $700^\circ\text{C}$ . *Economic Geology*, 61, 641-672.
- Sands, T., Washburn, J., and Gronsky, R. (1984) Interface morphology and phase distribution in the  $\text{Cu}_{2-x}\text{S}/\text{CdS}$  heterojunction: A transmission electron microscope investigation. *Solar Energy Materials*, 10, 349-370.
- Skinner, B.J. (1970) Stability of the tetragonal polymorph of  $\text{Cu}_2\text{S}$ . *Economic Geology*, 65, 724-730.
- Takeda, H., Donnay, J.D.H., and Appleman, D.E. (1967) Djurleite twinning. *Zeitschrift für Kristallographie*, 125, 414-422.
- Te Velde, T.S., and Dieleman, J. (1973) Photovoltaic efficiencies of copper-sulphide phases in the topotaxial heterojunction copper-sulphide-cadmium-sulphide. *Philips Research Reports*, 28, 573-595.
- Veblen, D.R. (1992) Electron microscopy applied to nonstoichiometry, polysomatism, and replacement reactions in minerals. In *Mineralogical Society of America Reviews in Mineralogy*, 27, 181-229.

MANUSCRIPT RECEIVED MAY 17, 1993

MANUSCRIPT ACCEPTED NOVEMBER 23, 1993